Influence of stacking-fault energy on the accommodation of severe shear strain in Cu-Al alloys during equal-channel angular pressing

Xianghai An, Qingyun Lin, and Shen Qu
Shenyang National Laboratory for Materials Science, Institute of Metal Research, Chinese Academy of Sciences, Shenyang 110016, China

Gang Yang
Central Iron and Steel Research Institute, Beijing 100081, China

Shiding Wu[a] and Zhe-Feng Zhang[b]
Shenyang National Laboratory for Materials Science, Institute of Metal Research, Chinese Academy of Sciences, Shenyang 110016, China

(Received 27 March 2009; accepted 29 June 2009)

X-ray diffraction (XRD) and transmission electron microscope (TEM) investigations have been carried out to decode the influence of stacking-fault energy (SFE) on the accommodation of large shear deformation in Cu-Al alloys subjected to one-pass equal-channel angular pressing. XRD results exhibit that the microstrain and density of dislocations initially increased with the reduction in the SFE, whereas they sharply decreased with a further decrease in SFE. By systematic TEM observations, we noticed that the accommodation mechanism of intense shear strain was gradually transformed from dislocation slip to deformation twin when SFE was lowered. Meanwhile, twin intersections and internal twins were also observed in the Cu-Al alloy with extremely low SFE. Due to the large external plastic deformation, microscale shear bands, as an inherent deformation mechanism, are increasingly significant to help carry the high local plasticity because low SFE facilitates the formation of shear bands.

I. INTRODUCTION

During the last two decades, bulk ultrafine grained (UFG) or nanocrystalline (NC) materials have been investigated extensively due to their new physical and enhanced mechanical properties.[1–3] Various approaches based on severe plastic deformation (SPD)-induced grain refinement have been developed for synthesizing UFG/NC materials, including equal-channel angular pressing (ECAP),[4–14] high-pressure torsion (HPT),[15–17] accumulative roll bonding (ARB),[18] low temperature rolling (LTR),[19] and dynamic plastic deformation (DPD).[20–22] Among them, ECAP is considered as one of the most important and efficient SPD methods to produce bulk UFG materials while maintaining their original geometry.[2]

As one of the major SPD methods, ECAP has been used to experimentally explore many materials with different crystallographic structures (fcc, bcc, and hcp), such as Al, Cu, Fe, and Ti.[4,6,9,23,24] A comprehensive understanding of grain-refinement mechanisms in these materials has been achieved by taking into account dislocation activity, deformation twinning, and phase transformation.[1,10,11,13] However, the influence of stacking-fault energy (SFE), one of the most important parameters in cubic structured materials, on the grain refinement and strain accommodation during ECAP is much less understood.[9,11,13]

In close-packed structures, SFE determines the extent of dislocation dissociation, affecting not only the dislocation substructures but also deformation behavior of the materials.[25–27] It has been well known that the higher the SFE, the smaller the separation between the partial dislocation and the thinner the stacking fault, and vice versa.[26,27] During plastic deformation of fcc metals, the partial dislocations move as a unit, maintaining the equilibrium width of the faulted region. Thus, in high/medium-SFE materials, cross-slip can readily occur by pinching the partial dislocations on their original slip plane and then recombining them to subsequently extend on the cross-slip plane due to small faulted region (high SFE).[26,27] Moreover, cross-slip, as a significant dynamic recovery mechanism, plays a crucial role in the rearrangement and annihilation of screw dislocations. Thus, this mechanism is incorporated in an explicit manner into all theories of pattern or the formation of cell-like structures in which the majority of the dislocations reside in cell walls and the interior of the cells is relatively dislocation-free.[28] On the other hand, in low-SFE

Address all correspondence to these authors:
[a]e-mail: shdwu@imr.ac.cn
[b]e-mail: zhfzhang@imr.ac.cn
DOI: 10.1557/JMR.2009.0426

materials, the large width of stacking fault increases the difficulty of recombining the partials into unit dislocation, limiting dislocation movement. Consequently, the restriction of cross-slip causes dislocations to organize themselves into planar arrays or planar slip bands (i.e., a more uniform dislocation distribution). In addition, the transition from high or medium to low SFE not only influences the slip mode from wavy to planar slip, but it also changes the mechanism of deformation from slip to twin. Twinning and slip are competitive deformation processes; in general, slip plays a dominating role at room temperature and at low strain rates in the high-/medium-SFE materials.[29] Twinning can contribute to the plastic deformation and to the slip mechanism only at high strain rates and/or at low temperatures. However, in those low-SFE materials, twinning readily occurs even during quasi-static deformation at room temperature.[26–29]

In previous investigations, most of the attention was focused on the materials with medium or high SFE, such as Al, Cu, and Ni.[4,5,30] In these materials, the SPD imposed by ECAP is dominantly accommodated by accumulation, interaction, tangling, and spatial rearrangement of dislocations. However, the strain accommodation and microstructures of the materials with low SFE subjected to ECAP are less informed.[10,12,13] More significantly, it was found that the mechanical behavior of UFG materials can be globally improved with lowering the SFE[11,13,17]; meanwhile, SFE is also a crucial factor to influence the prevailing plastic deformation and essentially affect the mechanical behaviors in nanocrystalline fcc metals.[31] Thus, it is thoroughly integrant to investigate the influence of SFE in both the strain accommodation and microstructure of the metals subjected to ECAP, which can provide fundamental scientific insight into the process of plastic deformation and help understand corresponding mechanical properties. Although the equivalent strain after one-pass ECAP can also be attained by conventional rolling or extrusion, the intense shearing provided by ECAP is a near "ideal" deformation method to achieve special structure, texture, and properties in comparison with conventional metal processing.[2] Herein, we attempt to study the microstructure variation and deformation mechanisms of three polycrystalline Cu-Al alloys with different SFE after one-pass ECAP, because repetitive pressings will change the strain path and involve more grain refinement that might make severe plastic deformation behavior difficult to analyze.

II. EXPERIMENTAL PROCEDURE

A. Samples and processing

Three Cu-Al alloys with different Al contents (Cu-2.3at.%Al, Cu-7.2at.%Al, and Cu-11.6at.%Al), initially obtained as a cold-drawn rod, were selected in this study. The SFEs of the three alloys are 48.5, 28, and 4.5 mJ/m^2,[11] respectively. Before pressing, the Cu-Al alloy rods were annealed at 800 °C for 2 h to diminish the effect of mechanical processing and obtain homogeneous microstructures. Subsequently, the annealed coarse-grained (CG) bars with 8-mm diameter and 45-mm length were used for the ECAP process. The ECAP procedure was performed by using a die fabricated from tool steel (AISI M4-like) with two channels intersecting at an inner angle of 90° and an outer angle of 30°, resulting in a large shear strain of ~1.[32] The rod coated with a MoS_2 lubricant was pressed for one pass at room temperature with a pressing speed of 9 mm/min.

B. Microstructure characterization

An electron channeling contrast (ECC) technique in a Cambridge S-360 scanning electron microscope (SEM; UK) was used to characterize the microstructure of the initial CG Cu-Al alloys. As shown in Fig. 1, the average grain size was estimated to be in the range of 300 to 400 μm excluding annealing twin boundaries by the linear intercept method, and annealing twins with micrometer-dimension lamellae were observed frequently.

After ECAP, x-ray diffraction (XRD) analysis of the as-deformed Cu-Al alloys was performed on the Y plane of the samples[2] by using a Rigaku DMAX/2400 x-ray diffractometer (Rigaku, Tokyo, Japan) with CuKα radiation [12 KW; wavelengths $\lambda_{K\alpha1}$ = 1.54056 Å and $\lambda_{K\alpha2}$ = 1.54439 Å were reflected by a graphite crystal using the (0002) reflection]. Microstrain of the samples was measured by means of XRD peak-broadening analysis by using the Scherrer-Wilson method.[33] Each datum point was averaged from two independent measurements. The microstructure characterization after ECAP processing was performed on transmission electron microscope (TEM) (JEM-2010; JEOL, Tokyo, Japan) operated at 200 kV and on FEI Tecnai F30 TEM (Eindhoven, The Netherlands) operated at 300 kV for high-resolution TEM (HRTEM). Thin foils for TEM observations, cut from the Y plane in the centers of the pressed rods, were then first mechanically ground to approximately 50-μm thick and finally thinned by a twin-jet polishing method in a solution of 25% phosphoric acid, 25% ethanol, and 50% water at a voltage of 8 to 10 V and at room temperature.

III. EXPERIMENTAL RESULTS

A. Microstrain

Microstrain measured from XRD peak broadening is shown in Fig. 2, which mainly represents the concentration of crystalline defects in the as-processed samples.[33] The microstrain increases from 0.13% for Cu-2.3at.%Al to 0.15% for Cu-7.2at.%Al, both of which are higher than the value (0.05%) of Cu subjected to one-pass ECAP.[5] It is evident that the microstrain significantly

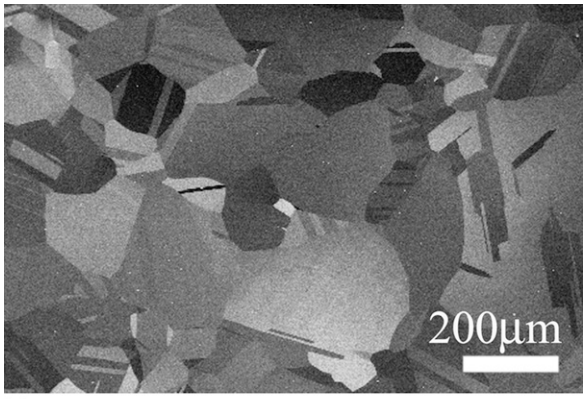

(a)

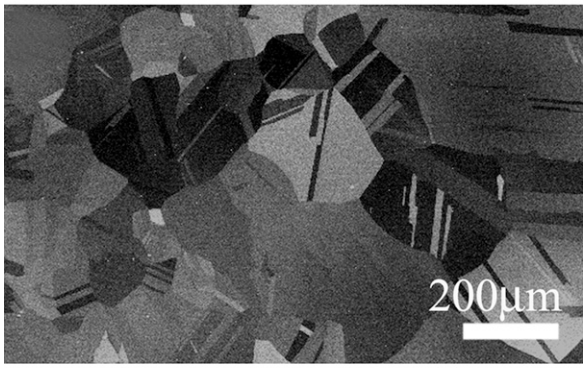

(b)

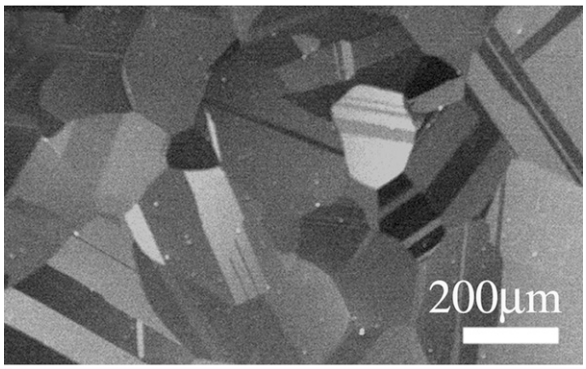

(c)

FIG. 1. SEM-ECC micrographs of annealed CG Cu-Al alloys: (a) Cu-2.3at.%Al; (b) Cu-7.2at.%Al; (c) Cu-11.6at.%Al.

increases with the introduction of Al (decreasing the SFE). However, with further increasing Al, the microstrain drastically decreased to 0.03% for Cu-11.6at.%Al, even lower than that of pure Cu. The general tendency of microstrain variation is consistent with the results of the Cu-Al alloys subjected to shock deformation.[34]

The dislocation density ρ can be closely related to the microstrain by $\rho = 16.1 \times \varepsilon^2/b^2$,[35] where ε is the microstrain and b is the Burgers vector. The evolution of dislocation density, consistent with that of the microstrain, initially increases from 4×10^{14} m^{-2} for Cu-2.3at.%Al to 5.7×10^{14} m^{-2} for Cu-7.2at.%Al, both of which are close to the previous data of previous

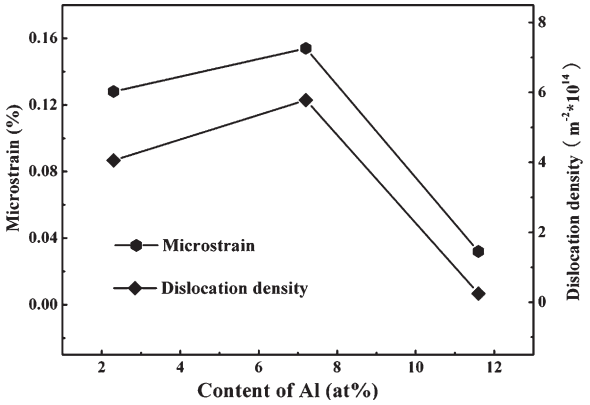

FIG. 2. Variation of measured microstrain and derived dislocation density from XRD analysis with the content of Al.

investigations derived from the XRD measurements.[1,2] Likewise, the dislocation density of Cu-11.6at.%Al sharply decreases to 2.5×10^{13} m^{-2}, obviously lower than the results of other fcc metals (such as Al, Cu, Ni) subjected to ECAP.[1] The reason for the decrease in the dislocation density may be attributed to the short-range order or due to the preferential formation of deformation twins in the low-SFE alloys.[34] The present data of dislocation density in Cu-11.6at.%Al is similar to that of pure Ti subjected to one-pass ECAP, the deformation of which was primarily accommodated via $\{10\bar{1}1\}$ mechanical twinning.[24] Owing to the extremely low SFE inhibiting the cross-slip, the reduction in dislocation density can be ascribed to the operation of deformation twinning rather than via dynamic recovery, which will be further confirmed in the following section.

B. TEM characterization

1. Microstructures of Cu-2.3at.%Al alloy after one-pass ECAP

Typical bright-field TEM micrographs of the microstructures of Cu-2.3at.%Al alloy subjected to one-pass ECAP are presented in Fig. 3. Analogous with the major microstructure characters of Al and Cu after the first ECAP pass, it mainly consists of parallel extended planar dislocation boundaries [geometrically necessary boundaries (GNBs)] and randomly oriented cell boundaries [incidental dislocation boundaries (IDBs)]. These lamellar GNBs, with average spacing of approximately 200 nm, form between the regions of different strain patterns to accommodate the glide-induced lattice rotation due to large accumulated differences in the slip system activity or slip pattern on either side of the boundary, whereas the formation of IDBs stems from random trapping and tangling of dislocations that do not cause a significant rotation of the lattice.[36] A small misorientation across GNBs was noticed from the selected-area electron diffraction (SAED), indicating that dislocation density

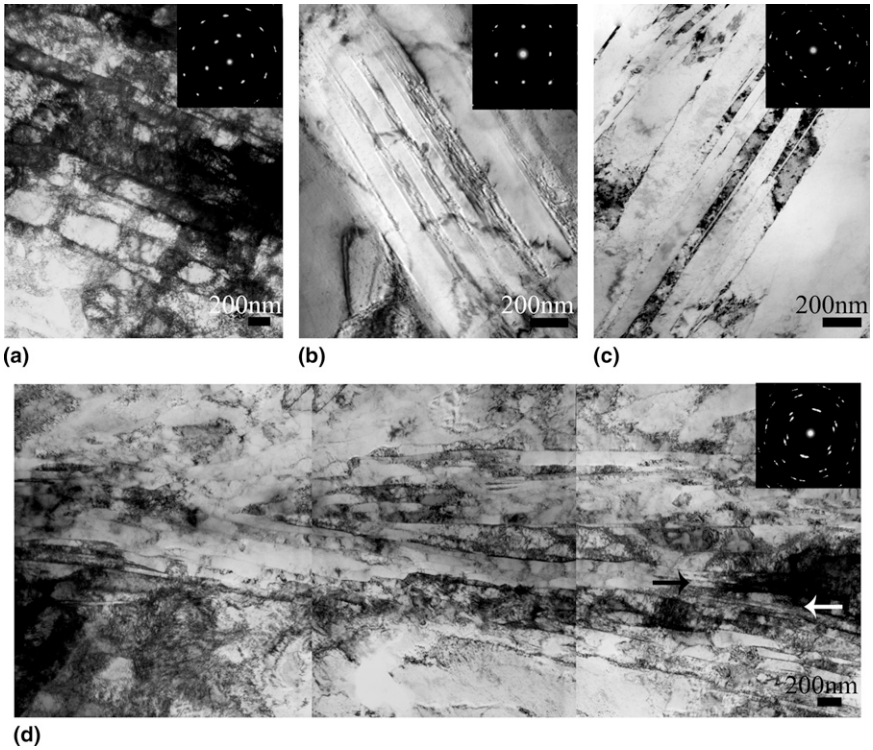

FIG. 3. TEM micrographs of microstructures of Cu-2.3at.%Al alloy after ECA pressing for one pass: (a) parallel lamellar boundaries; (b) stacking fault observed from [001] diffraction; (c) deformation twins; (d) microscale shear bands and the SAED are related to the region marked by the white and black arrows.

accommodating the lattice rotation in the boundaries is high. The inhomogeneous deformation reflects the presence of plastic strain gradients.[37,38]

Other than the extensive dislocation activities, some deformation twins and stacking faults in several grains can help carry the severe plastic deformation in Cu-2.3at.%Al alloy, as demonstrated in Figs. 3(b) and 3(c). Unlike the formation of deformation twins localized in shear bands and their intersections in pure Cu subjected to ECAP,[8] twin-matrix (T-M) lamellae formed due to its relatively low SFE although the density of deformation twins is low. Moreover, thanks to the intense shear during ECAP, several copper-type shear bands formed against a background of band-like dislocation structures of elongated cells in some regions, as exhibited in Fig. 3(d). The formation of these microscale shear bands originated from the rotation of previously formed microbands and made themselves parallel to the macroscopic stress axes and cluster together to form bundles.[39] Similar to the observations in Cu,[8] deformation twins formed in these bands but are limited to a narrow region marked in Fig. 3(d), and dislocation slip dominated the plastic deformation through the formation of elongated subgrains in the other areas. Thus, dislocation slip is the most crucial deformation mode for bearing the intense shear strain in Cu-2.3at.%Al alloy, although several deformation twins, stacking faults, and shear bands were formed.

2. Microstructures of Cu-7.2at.%Al alloy after one-pass ECAP

The salient features of deformed microstructures in Cu-7.2at.%Al alloy are exhibited in Figs. 4 and 5. The aligned GNBs intersected by thin shear bands within some grains are shown in Fig. 4(a), and they have been termed "S-bands" due to the "S" shape, which is similar to those reported in extensively rolled Al and Cu.[28] In these grains, dislocation activities still play essential roles in the plastic deformation, whereas the density of shear bands in Cu-7.2at.%Al alloy are higher than that in Cu-2.3at.%Al alloy. It may signal that more shear bands are operated to help undertake the severe plastic deformation due to the decreased dislocation activities resulting from the reduction in SFE of the alloy. Meanwhile, dislocation planar slip can be found forming planar band structures in some areas, and the intersections of band structures were also observed due to operation of different slip systems in Fig. 4(b). The coexistence of two types of dislocation substructures is consistent with the prediction that both of them can be found when Al content is in the range of approximately 6 at.% ~9 at.%.[40]

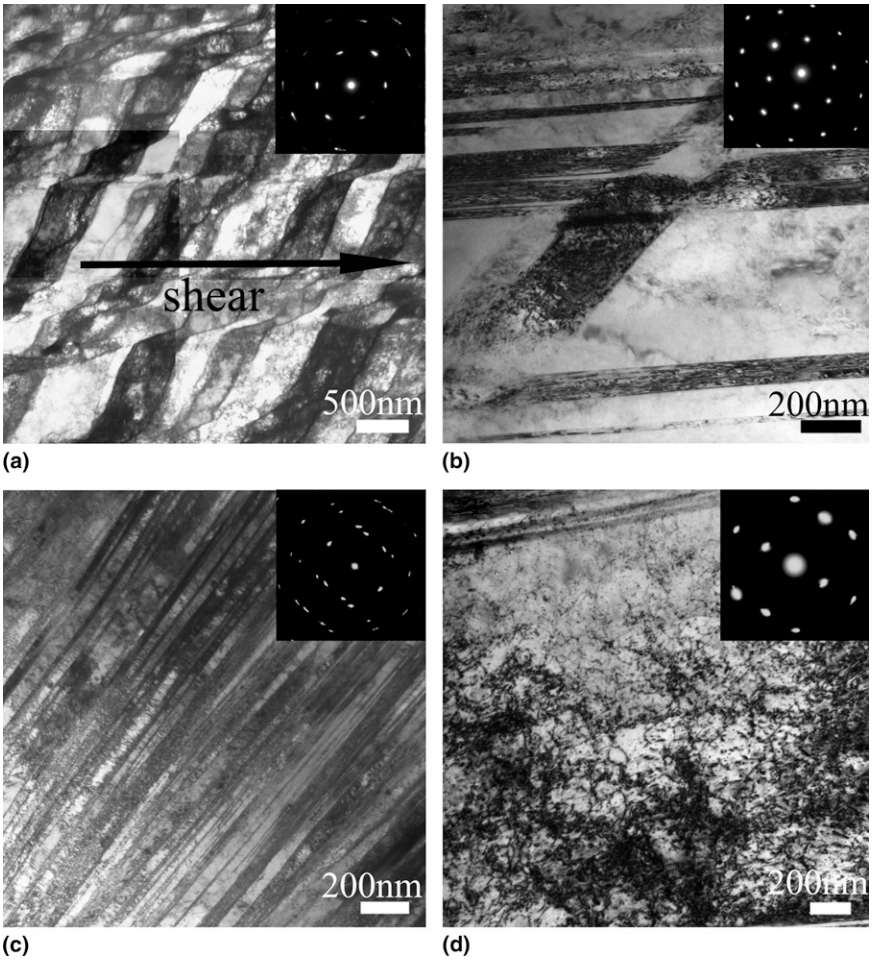

FIG. 4. TEM micrographs of microstructures of Cu-7.2at.%Al alloy after ECAP for one pass: (a) S bands; (b) profuse deformation twins; (c) dislocation morphologies between T-M lamellae.

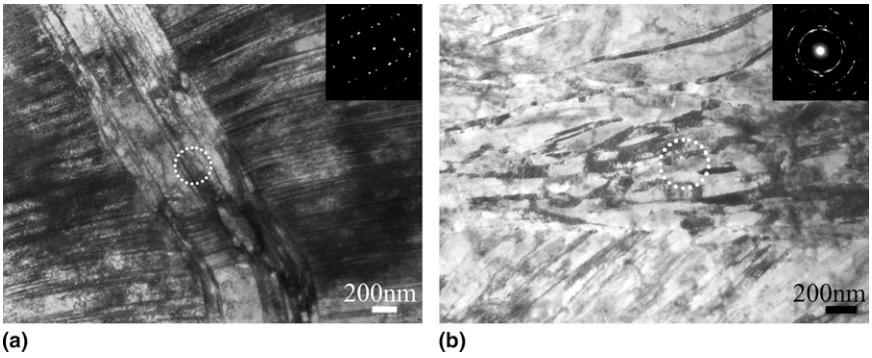

FIG. 5. Typical TEM imagines of brass-type shear band, within which different microstructures are shown: (a) deformation twin and (b) elongated subgrains in the shear bands.

In addition to dislocation movements in some areas, the most pronounced microstructure characteristic of the Cu-7.2at.%Al alloy is the formation of profuse deformation twins with the thickness of several tens of nanometers in many grains. Meanwhile, high-density dislocations were located at the T-M lamellae, implying that the large stress concentration in these regions and complicated dislocation configuration was also detected between T-M lamellae, as shown in Fig. 4(d). Thus, both complicated dislocation activities and profuse deformation twins are significantly essential to accommodate the intense plastic deformation in Cu-7.2at.%Al.

Other than these two common deformation modes, shear bands play more remarkable roles in carrying the shear strain with the decrease of SFE.[39] Different from the copper-type shear bands observed in Figs. 3(d) and

4(a), many "brass-type" shear bands with width of ~400 nm, often formed in the metals with medium/low SFE in which deformation twinning becomes an essential deformation mechanism, can be detected as indicated in Fig. 5. Although the formation background of the brass-type shear band is similar, various microstructures within the shear bands are exhibited, which may be related to the evolution degree of shear bands. As delineated in Fig. 5(a), many small mechanical twins parallel to the direction of shear bands were found and proved by the SAED from the region marked by dotted circle. In this case, the development of shear bands may be in the early stage in which the (111) twinning planes are progressively rotated into a position parallel to the shear plane by the shear bands.[41] In contrast, in a well developed band, its microstructure is mainly composed of fine subgrains, slightly elongated along the shear direction, as shown in Fig. 5(b). As mentioned above, the density of shear bands remarkably increases with the reduction of SFE, indicating that they are more significant as the complementary deformation mode besides dislocations slip and deformation twins.

3. Microstructures of Cu-11.6at.%Al alloy after one-pass ECAP

Figures 6–8 manifest the prominent microstructural morphologies of the Cu-11.6at.%Al alloy with extremely low SFE after one-pass ECAP process. Pronounced dislocation slip features can be found in few grains in which plenty of dislocations are trapped by the banding structures resulting in the planar arrays, as shown in Fig. 6(a). The corresponding SAED pattern reveals the small misorientation between these bands, and it is interesting to note that no deformation twins existed in these areas even though the SFE of Cu-11.6at.%Al alloy is low. However, in most regions of the alloy, a high density of deformation twins formed, delineated in Fig. 6(b), homogeneously transforming the deformed Cu-11.6at.% Al alloy into a laminar structure of fine, alternating T-M layers. Although amounts of dislocations also reside in the twinned area, its density is apparently lower than that in Cu-7.2at.%Al alloy according to the image contrast observation. Meanwhile, Fig. 6(c) exhibits that profuse stacking faults can be observed from the [001] direction. Moreover, nearly all the brass-type shear bands are well developed, and its density is obviously higher than that in Cu-7.2at.%Al alloy, as discerned in Fig. 6(d). The microstructure in the region of shear bands is very fine and mainly consists of nanoscale grains, and the corresponding SAED patterns from the area marked by dotted circles show that the nanograins are uniformly distributed in these bands.

The occurrence of twin-twin intersections indicates that different twinning systems were activated during the severe shear deformation in some areas, and the corresponding SAED pattern demonstrates that the intersection angle of two twin systems is approximately 70°, as shown in Fig. 7(a). The HRTEM observations, exhibited in Fig. 7(b), reveal that primary twinning system

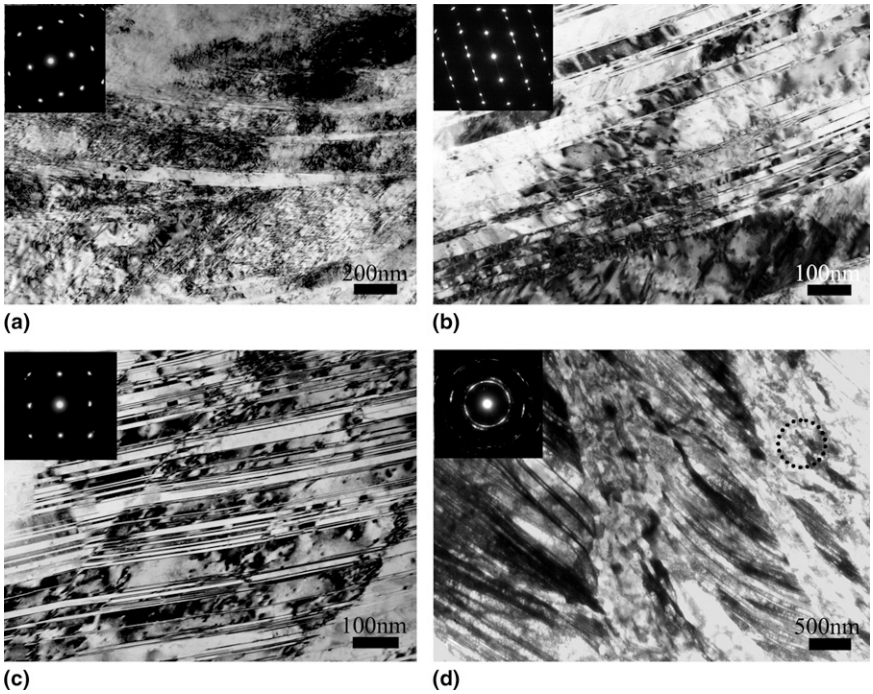

FIG. 6. TEM micrographs of microstructures of Cu-11.6at.%Al alloy after ECAP for one pass: (a) planar dislocation configuration; (b) profuse deformation twins; (c) amounts of stacking fault observed from [001] diffraction; (d) nanograins formed in shear band.

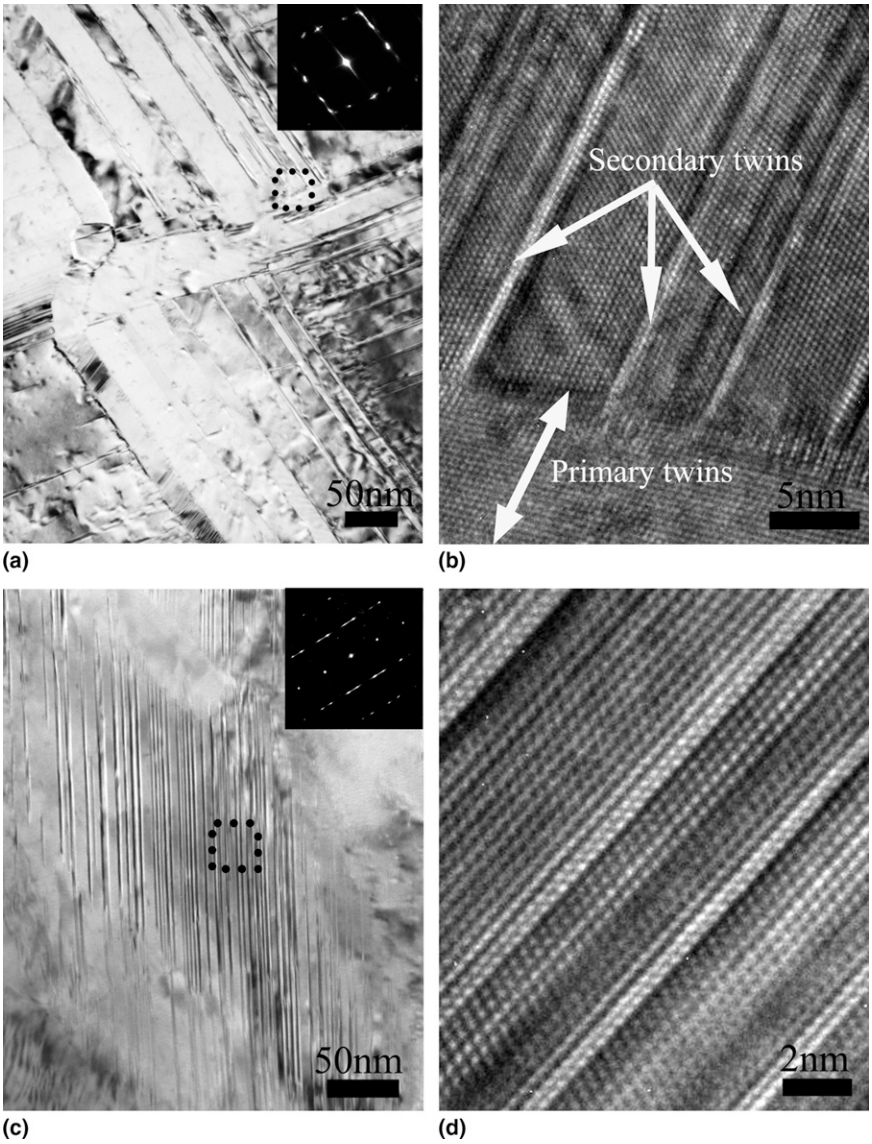

FIG. 7. (a) Bright TEM imagine of twin-twin intersection formed in Cu-11.6at.%Al alloy; (b) the [011] HRTEM micrographs corresponding the region marked in (a); (c) typical TEM micrograph of stacking fault embedded in T-M lamellae observed from [011] direction; (d) [011] HRTEM image of the area marked in (c).

noticeably governs the initial deformation region, and the existing primary twins block the propagation of secondary twins by restricting the mean free path of the twin dislocations.[27] Moreover, as manifested in Fig. 7(c), another salient feature in the twinned regions is many stacking faults embedded inside the T-M lamellae, which was proved by several streaks exhibited in the SAED pattern. In Fig. 7(d), the HRTEM image of the area marked in Fig. 7(c) also demonstrated that profuse stacking faults embedded in the twinned areas. As the embryos of deformation twins, the stacking faults are formed by the dissociation of dislocations into partials and will lead to the formation of abundant twins under external driving stress. The existence of many stacking faults in the T-M lamellae may be ascribed to the high density of twins, and, as a result, there is not enough room for the expansion of stacking faults.

Profuse internal twins, a pattern of secondary twins within a primary twin, were found as shown in Fig. 8, which was also observed in austenitic steels.[42] The angle of the primary twins and the internal twins, measured by the SAED patterns, is similar to that of twin intersection, $\sim 70^{\circ}$. It is proposed that internal twining may be an essentially collective dislocation process leading to the simultaneous development of primary and secondary twins[42]; however, it is also argued that the rigid body rotation of the sample makes the crystallographic orientation of another twinning system satisfy the requirement of critical shear stress to activate the secondary twin due to the complicated deformation mode of ECAP.[14] As a

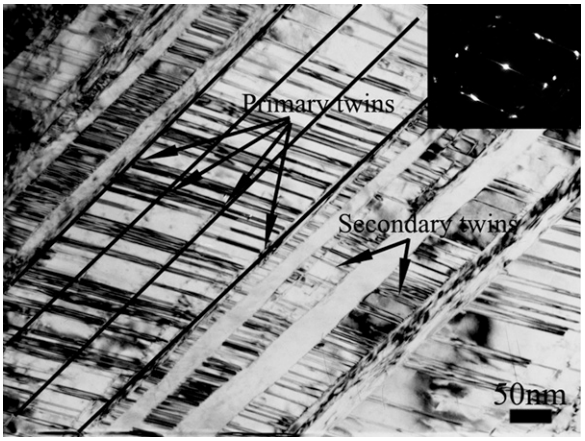

FIG. 8. A typical TEM image containing profuse internal twins. The primary twins and internal twins are marked by arrows.

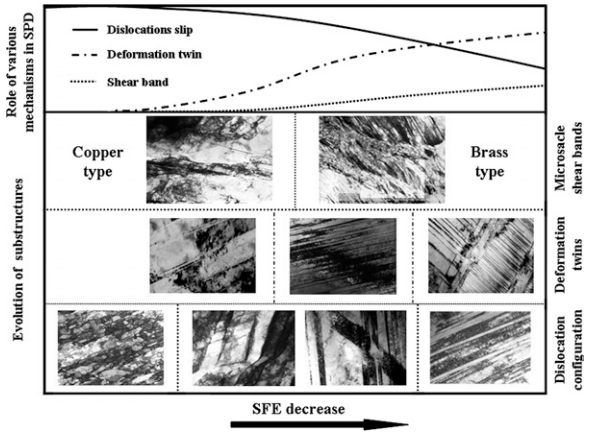

FIG. 9. Schematic diagram showing the influence of SFE on the evolution of dislocation configuration, deformation twins, and shear bands in Cu-Al alloy during severe plastic deformation.

result, the resultant microstructures of Cu-11.6at.%Al alloy with extremely low SFE after one-pass ECAP signal that the intense shear deformation imposed by SPD is dominantly accommodated by the deformation twins, although dislocation slip is firstly operated in a few grains, and the role of shear bands in the plastic deformation is increasingly significant.

IV. DISCUSSION

When plastic deformation was imposed on the materials, dislocation can be generated, moved by the sliding blocks of the crystals over one another along definite crystallographic planes and closed-packed direction. However, consideration of the atomistic arrangement on the {111} plane of fcc crystals, unit dislocations should be dissociated into partial dislocations for lowering their energies, which is the energetically favorable process to accomplish the slip and produce the stacking fault between the partials.[25–27] Thus, as mentioned above, because the movement of the partials is restricted to a specific slip plane to maintain the equilibrium separation between them determined primarily by SFE, an extended screw dislocation cannot cross-slip unless the partial dislocations recombine into a perfect dislocation.[27] This result implies that SFE is the most essential factor to influence the dislocation substructures. As shown in Fig. 9, with the reduction in the SFE, the dislocation configurations are gradually transformed from wavy slip in the Cu-2.3at.%Al alloy to mixed dislocation structures consisting of both wavy and planar arrangement in the Cu-7.2at.%Al, and they can finally be arranged into planar arrays in the Cu-11.6at.%Al, which is consistent with the previous investigation.[40]

In fact, dislocation sources will be activated to carry the shear strain in the onset of plastic deformation due to the low critical resolved shear stress. In general, two kinds of dislocations can be distinguished and classified into statistically stored dislocations (SSDs) and geometrically necessary dislocations (GNDs).[36,37] The former is accumulated by trapping each other in a random way under the uniform deformation; the latter generally develops to ensure the compatibility of deformation and accommodate the shear strain gradients in various parts of the materials suffering inhomogeneous deformation.[37] With an increase in the plastic strain, the chances of mutual trapping and/or annihilation of dislocations increase due to the active motions of dislocations in the high-/medium-SFE materials. Therefore, dislocations are assembled into boundaries to maintain the low-energy dislocation structures.[43] Consequently, the GNBs and IDBs, which derived from the GNDs and the SSDs, respectively, are developed to bear the large plastic strain including the homogeneous and the heterogeneous, as exhibited in Cu-2.3at.%Al alloy in which the dislocation activities are the most remarkable mechanism to bear the plastic deformation. Instead of the formation of IDBs and GNBs, banded, linear arrays of dislocations can be observed in Cu-7.2at.%Al and Cu-11.6at.%Al with low SFE due to the confinement of dislocations movement; meanwhile, the short-range order (SRO) of solid solution atoms may also trigger the planar slip formation.[40] Thus, the reduced ability of dislocation activities and SRO promote the planarity of slip, arranging the dislocations into parallel bands to uniformly accommodate the plastic deformation, as shown in Figs. 4(b) and 6(a).

More significantly, not only dislocation configurations but also plastic deformation accommodation mechanisms are gradually transitional with decrease of the SFE as illustrated in Fig. 9. As mentioned above, the low SFE inhibits the cross-slip and reduces the dislocation activities; thus, only dislocation slip cannot sufficiently hold the macroscopic or mesoscopic plastic strain

gradients including those externally imposed and ones arising from the heterogeneity of the microstructures. As another essential deformation mode, deformation twinning is more favorable in the materials with low SFE; therefore, it should become the most prominent undertaker of the plastic deformation in Cu-7.2at.%Al and Cu-11.6at.%Al due to the reduction in the critical twining stress, as exhibited in Fig. 9. Although SRO increases the stress required for twinning because twinning dislocations in successive twinning planes have to pass through the SRO, the critical resolved shear stress for twinning in fcc metals is predominantly influenced by the SFE of materials.[25] Thus, the strain gradients will mainly be accommodated by the storage of an extra density of deformation twins rather than mainly by GNDs or GNBs in the fcc metals with low SFE. For example, in Cu-7.2at.%Al with low SFE, deformation twins begin to play significant roles in the large shear strain, although two types of dislocation configurations coexist and high density of dislocations reside in the formed T-M lamellae. With a further decrease of SFE, profuse deformation twins, taking the place of dislocation slip, become the dominating plastic mechanism to accommodate the large strain gradients in Cu-11.6at.% Al alloy. Meanwhile, the twin intersection and internal twins are activated to help carry the SPD, although dislocation slip is first activated in few grains, the crystallographic orientation of which is extremely unfavorable for twinning.[14,29] Therefore, the plastic deformation accommodation mechanism is, step-by-step, transformed from a dislocation slip-dominated to a deformation twin-dominated one with the reduction in SFE of alloys.

With the normal crystallographic deformation processes precluded, a state of plastic instability and extensive localization develops in terms of shear bands. Although the shear banding is generally considered as a failure mode in some brittle materials,[44] on the scale of grains, this shear localization and instability become an inherent feature of plastic deformation when extensive strain under highly constrained conditions such as ECAP was imposed. According to the values of SFE, two kinds of shear bands can be distinguished and classified into "copper-type" and "brass-type" ones,[13] and it is well established that a low SFE and/or deformation temperature strongly facilitates the formation of shear bands,[28,38,40] which is consistent with the present experimental results: the density of shear band increased when the SFE is reduced. In Cu-2.3at.%Al alloy, the copper-type shear bands stem from the rigid rotation of the microbands but are not related to the crystalline morphology at high strain level to help accommodate the large plastic strain gradients. However, in Cu-11.6at.% Al alloy, due to its extremely low SFE, most grains may be uniformly twinned and twins cluster together, forming some banded regions at the early stage of pressing, i.e., entering the deformation zone.[6] With further increasing strain especially during the sample passing the main plane, the shear bands begin to develop to bear the inhomogeneous deformation because the twin and matrix elements of the structure are so thin that normal slip processes cannot occur due to the high frequency with which the dislocations encounter boundaries. Thus, as demonstrated in Fig. 9, the role of shear band in undertaking the large plastic deformation becomes increasingly important with the decrease of the SFE.

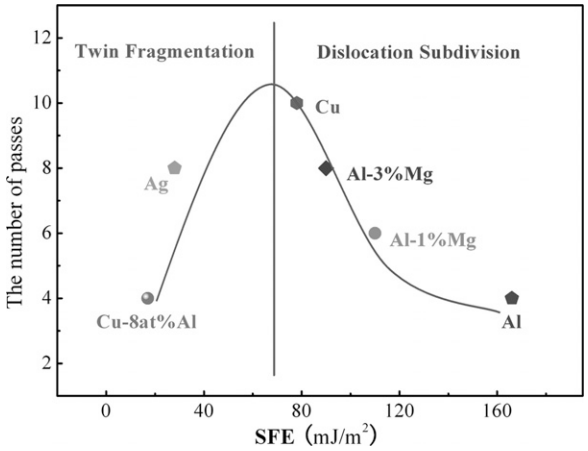

FIG. 10. Relationship between the numbers of ECAP passes required for homogeneous microstructures and the SFE, indicating the transformation of the grain refinement mechanism from dislocation subdivision to twin fragmentation.[9,13,45]

Systematic investigations about the influence of SFE on the large shear strain accommodation are crucial to comprehensively understand the microstructure evolution and grain refinement mechanism during ECAP. It is well established that the grain refinement of single-phase metals during SPD is via dislocation activities or deformation twins, which is closely related to the SFE. As illustrated in Fig. 10, the degree of microstructure evolution during ECAP is also closely related to the influence of SFE, which has been discussed in detailed elsewhere,[13] and the grain refinement mechanism is gradually transformed from dislocation subdivision for the high/medium-SFE materials to twin fragmentation for the low-SFE materials.[13] More essentially, unveiling the role of SFE in the microstructure evolution not only provides us with an excellent opportunity to profoundly comprehend the nature of grain refinement mechanism and to extend our understanding of the structure-properties relationship of UFG/NC materials processed by SPD,[11,13] but it also provides an attractive potential to prepare UFG/NC materials with excellent mechanical properties for technological applications.

V. CONCLUDING REMARKS

It is clear from our detailed investigation that we uncovered the influence of SFE as one of the most

crucial parameters in the cubic-structured materials on the microstructure after ECAP, and we disclosed the apparently different roles of dislocation slip, deformation twins, and microscale shear bands in bearing large shear deformation by tailoring the SFE of the materials.

The microstrain and dislocation density derived from the XRD, to some extent, signal the transformation of shear strain accommodation. By the systematic TEM observations, it can be found that the undertaker of large plastic strain gradients is gradually transformed from dislocation activities dominated in Cu-2.3at.%Al to a deformation twin-dominated one in Cu-11.6at.%Al with the reduction in the SFE. In addition, the higher dislocation density in Cu-7.2at.%Al compared to that in Cu-2.3at.%Al can be attributed to the formation of deformation twins, which restricts the dislocation activities and the decreased ability of cross-slip, making the arrangement and annihilation of dislocations difficult. However, in Cu-11.6at.%Al with extremely low SFE, profuse thin deformation twins, predominantly accommodating the intense shear strain, make the slip difficult, resulting in the decrease of dislocation density. Other than the two crystallographic deformation modes, microscale shear bands play an increasingly essential role in the large plastic deformation when SFE is decreased.

ACKNOWLEDGMENTS

This work was supported by National Natural Science Foundation of China (NSFC) under Grant Nos. 50841024 and 50890173. Z.F.Z. would like to acknowledge the "Hundred of Talents Project" by Chinese Academy of Sciences and the National Outstanding Young Scientist Foundation (under Grant No. 50625103) for financial support.

REFERENCES

1. R.Z. Valiev, R.K. Islamgaliev, and I.V. Alexandrov: Bulk nanostructured materials from severe plastic deformation. *Prog. Mater. Sci*. **45,** 103 (2000).
2. R.Z. Valiev and T.G. Langdon: Principles of equal-channel angular pressing as a processing tool for grain refinement. *Prog. Mater. Sci*. **51,** 881 (2006).
3. H. Gleiter: Nanostructured materials: Basic concepts and microstructure. *Acta Mater*. **48,** 1 (2000).
4. Y. Iwahashi, Z. Horita, M. Nemoto, and T.G. Langdon: The process of grain refinement in equal-channel angular pressing. *Acta Mater*. **46,** 3317 (1998).
5. F. Dalla Torre, R. Lapovok, J. Sandlin, P.F. Thomson, C.H.J. Davies, and E.V. Pereloma: Microstructures and properties of copper processed by equal channel angular extrusion for 1–16 passes. *Acta Mater*. **52,** 4819 (2004).
6. Q. Xue, I.J. Beyerlein, D.J. Alexander, and G.T. Gray III: Mechanisms for initial grain refinement in OFHC copper during equal channel angular pressing. *Acta Mater*. **55,** 655 (2007).
7. W.Z. Han, Z.F. Zhang, S.D. Wu, and S.X. Li: Influences of crystallographic orientations on deformation mechanism and grain refinement of Al single crystals subjected to one-pass equal-channel angular pressing. *Acta Mater*. **55,** 5889 (2007).
8. C.X. Huang, K. Wang, S.D. Wu, Z.F. Zhang, G.Y. Li, and S.X. Li: Deformation twinning in polycrystalline copper at room temperature and low strain rate. *Acta Mater*. **54,** 655 (2006).
9. S. Komura, Z. Horita, and M. Nemoto: Influence of stacking fault energy on microstructural development in equal channel angular pressing. *J. Mater. Res*. **14,** 4044 (1999).
10. C.X. Huang, Y.L. Gao, G. Yang, S.D. Wu, G.Y. Li, and S.X. Li: Bulk nanocrystalline stainless steel fabricated by equal channel angular pressing. *J. Mater. Res*. **21,** 1687 (2006).
11. X.H. An, W.Z. Han, C.X. Huang, P. Zhang, G. Yang, S.D. Wu, and Z.F. Zhang: High strength and utilizable ductility of bulk ultrafine-grained Cu–Al alloys. *Appl. Phys. Lett*. **92,** 201915 (2008).
12. G.G. Yapici, I. Karaman, Z.P. Luo, H.J. Maier, and Y.I. Chumlyakov: Microstructural refinement and deformation twinning during severe plastic deformation of 316L stainless steel at high temperatures. *J. Mater. Res*. **19,** 2268 (2004).
13. S. Qu, X.H. An, H.J. Yang, C.X. Huang, G. Yang, Q.S. Zang, Z.G. Wang, S.D. Wu, and Z.F. Zhang: Microstructural evolution and mechanical properties of Cu–Al alloys subjected to equal channel angular pressing. *Acta Mater*. **57,** 1586 (2009).
14. W.Z. Han, S.D. Wu, C.X. Huang, S.X. Li, and Z.F. Zhang: Orientation design for enhancing deformation twinning in Cu single crystal subjected to equal channel angular pressing. *Adv. Eng. Mater*. **10,** 1110 (2008).
15. A.P. Zhilyaev, G.V. Nurislamova, B-K. Kim, M.D. Baró, J.A. Szpunar, and T.G. Langdon: Experimental parameters influencing grain refinement and microstructural evolution during high-pressure torsion. *Acta Mater*. **51,** 753 (2003).
16. C. Xu, Z. Horita, and T.G. Langdon: The evolution of homogeneity in processing by high-pressure torsion. *Acta Mater*. **55,** 203 (2007).
17. Y.H. Zhao, Y.T. Zhu, X.Z. Liao, Z. Horita, and T.G. Langdon: Tailoring stacking fault energy for high ductility and high strength in ultrafine grained Cu and its alloy. *Appl. Phys. Lett*. **89,** 121906 (2006).
18. Y. Saito, H. Utsunomiya, N. Tsuji, and T. Sakai: Novel ultra-high straining process for bulk materials—Development of the accumulative roll-bonding (ARB) process. *Acta Mater*. **47,** 579 (1999).
19. Y.M. Wang, M.W. Chen, H.W. Sheng, and E. Ma: Nanocrystalline grain structures developed in commercial purity Cu by low-temperature cold rolling. *J. Mater. Res*. **17,** 3004 (2002).
20. Y.S. Li, N.R. Tao, and K. Lu: Microstructural evolution and nanostructure formation in copper during dynamic plastic deformation at cryogenic temperatures. *Acta Mater*. **56,** 230 (2008).
21. Y. Zhang, N.R. Tao, and K. Lu: Mechanical properties and rolling behaviors of nano-grained copper with embedded nano-twin bundles. *Acta Mater*. **56,** 2429 (2008).
22. Y.S. Li, Y. Zhang, N.R. Tao, and K. Lu: Effect of the Zener–Hollomon parameter on the microstructures and mechanical properties of Cu subjected to plastic deformation. *Acta Mater*. **57,** 761 (2009).
23. B.Q. Han, F.A. Mohamed, and E.J. Lavernia: Mechanical properties of iron processed by severe plastic deformation. *Metall. Mater. Trans. A* **34,** 71 (2003).
24. D.H. Shin, I. Kim, J. Kim, Y.S. Kim, and S.L. Semiatin: Microstructure development during equal-channel angular pressing of titanium. *Acta Mater*. **51,** 983 (2003).
25. M.A. Meyers and K.K. Chawla: *Mechanical Behavior of Materials* (Prentice Hall, NJ, 1999).
26. G.E. Dieter: *Mechanical Metallurgy*, 3rd ed. (McGraw-Hill, Boston, 1986).
27. J.P. Hirth: *Theory of Dislocation*, 2nd ed. (John Wiley & Sons, 1982).
28. F.J. Humphreys and M. Hatherly: *Recrystallization and Related Annealing Phenomena*, 2nd ed. (Elsevier, Oxford, 2004).

29. W.Z. Han, Z.F. Zhang, S.D. Wu, and S.X. Li: Combined effects of crystallographic orientation, stacking fault energy and grain size on deformation twinning in FCC crystals. *Philos. Mag.* **88,** 3011 (2008).
30. A.P. Zhilyaev, B-K. Kim, J.A. Szpunar, M.D. Baró, and T.G. Langdon: The microstructural characteristics of ultrafine-grained nickel. *Mater. Sci. Eng., A* **391,** 377 (2005).
31. Z.W. Wang, Y.B. Wang, X.Z. Liao, Y.H. Zhao, E.J. Lavernia, Y.T. Zhu, Z. Horita, and T.G. Langdon: Influence of stacking fault energy on deformation mechanism and dislocation storage capacity in ultrafine-grained materials. *Scr. Mater.* **60,** 52 (2009).
32. Y. Iwahashi, J.T. Wang, Z. Horita, M. Nemoto, and T.G. Langdon: Principle of equal-channel angular pressing for the processing of ultra-fine grained materials. *Scr. Mater.* **35,** 143 (1996).
33. H.P. Klug and L.E. Alexander: *Diffraction Procedures for Polycrystalline and Amorphous Materials* (Wiley, New York, 1974).
34. A. Rohatgi and K.S. Vecchio: The variation of dislocation density as a function of the stacking fault energy in shock-deformed FCC materials. *Mater. Sci. Eng., A* **328,** 256 (2002).
35. G.K. Williamson and R.E. Smallman: Dislocation densities in some annealed and cold-worked metals from measurements on the x-ray Debye-Scherrer spectrum. *Philos. Mag.* **1,** 34 (1956).
36. D.A. Hughes, N. Hansen, and D.J. Bammann: Geometrically necessary boundaries, incidental dislocation boundaries and geometrically necessary dislocations. *Scr. Mater.* **48,** 147 (2003).
37. M.F. Ashby: The deformation of plastically non-homogeneous materials. *Philos. Mag.* **21,** 399 (1970).
38. H. Gao, Y. Huang, W.D. Nix, and J.W. Hutchinson: Mechanism-based strain gradient plasticity—I. Theory. *J. Mech. Phys. Solids* **47,** 1263 (1999).
39. M. Hatherly and A.S. Malin: Deformation of copper and low stacking-fault energy, copper base alloys. *Met. Tech.* **6,** 308 (1979).
40. S.I. Hong: Cyclic stress-strain response and slip mode modification in fatigue of f.c.c. solid solutions. *Scr. Mater.* **44,** 995 (2001).
41. H. Paul, J.H. Driver, and Z. Jasieński: Shear banding and recrystallization nucleation in a Cu–2%Al alloy single crystal. *Acta Mater.* **50,** 815 (2002).
42. P. Müllner and A.E. Romanov: Internal twinning in deformation twinning. *Acta Mater.* **48,** 2323 (2000).
43. D. Kuhlmann-Wilsdorf: Theory of plastic deformation: Properties of low-energy dislocation structures. *Mater. Sci. Eng., A* **113,** 1 (1989).
44. D. Kuhlmann-Wilsdorf: Deformation bands, the LEDS theory, and their importance in texture development: Part II. Theoretical conclusions. *Metall. Mater. Trans. A* **35,** 369 (2004).
45. J. Gubicza, N.Q. Chinh, J.L. Lábár, Z. Hegedüs, C. Xu, and T.G. Langdon: Microstructure and yield strength of severely deformed silver. *Scr. Mater.* **58,** 775 (2008).